Article

Nanostructured Zeolites: The Introduction of Intracrystalline Mesoporosity in Basic Faujasite-Type Catalysts

Aqeel Al-Ani, Richard John Darton, Scott Sneddon, and Vladimir I. Zholobenko

ACS Appl. Nano Mater., **Just Accepted Manuscript** • DOI: 10.1021/acsanm.7b00169 • Publication Date (Web): 21 Dec 2017

Nanostructured Zeolites: The Introduction of Intracrystalline Mesoporosity in Basic Faujasite-Type Catalysts

Aqeel Al-Ani [a]*; Richard J. Darton [a]; Scott Sneddon [a] ;Vladimir Zholobenko [a]*

[a] School of Chemical and Physical Sciences, Keele University, Keele, Staffordshire, ST5 5BG, United Kingdom

Abstract

A combination of post-synthesis modifications and ion-exchange aiming to obtain basic cation-rich hierarchical zeolites X and Y was utilised in this work for the preparation of catalysts for biofuel production from vegetable oils. The secondary mesopore system with a narrow pore size distribution in the 4 nm range was introduced by successive acid and base treatments accompanied with surfactant templating. This was followed by ion-exchange with Cs^+ and K^+ cations to produce strong basic catalysts. The prepared hierarchical zeolites have been characterised by X-ray diffraction (XRD), scanning electron microscopy (SEM), nitrogen adsorption, Fourier transform infrared spectroscopy (FTIR) and solid state NMR. The transesterification reaction over the zeolite catalysts was carried out in a microwave batch-type reactor and the effects of the reaction conditions, basic properties and pore structure of the hierarchical faujasites were studied in details. The conversion of triglycerides increased with increasing concentration of Cs and K in modified zeolites, but declined with decreasing framework aluminium content. The balance between the strength of the basic sites and their accessibility in hierarchical zeolites and its effect on the catalytic performance of these nanostructured materials is discussed.

Keywords: basic zeolite catalysts, hierarchical faujasites, structural characterisation, transesterification, surfactant, microwave catalysis

* Corresponding authors: Aqeel Al-Ani, e-mail address: a.a.t.al-ani@keele.ac.uk

Vladimir Zholobenko, e-mail address: v.l.zholobenko@keele.ac.uk

1. Introduction

For many decades zeolites have been utilised in a wide range of important catalytic applications due to the presence of strong acid sites, high surface area, shape selectivity and their unique molecular sieving properties [1-5]. Although microporosity is an essential feature of the conventional zeolites being associated with their molecular sieving properties and shape-selectivity, these types of catalysts can suffer from slow intracrystalline diffusion of bulky molecules inside the pores and limited accessibility of active sites [6-8]. In this respect, the considerable advances in the synthesis of novel structures, pore size engineering, preparation of nano-zeolites, hierarchical and hybrid structures have been instrumental in addressing the mass transfer limitations and enhancing the catalytic activity of zeolites and related materials [5,9-19]. Many of these approaches aiming to obtain hierarchical zeolites, which have multilevel pore architectures (including micro- and meso- and macro-pores), with strong acidity, high degree of crystallinity and improved diffusion properties have been broadly divided into two categories: (1) the so-called "top-down" strategy, e.g. developing secondary macro- and mesoporosity in zeolites by post-synthesis treatments leading to their structural re-arrangement involving dealumination and desilication; and (2) the "bottom-up" strategy, which can be based on the application of "hard" or "soft" templating during the zeolite synthesis to introduce particular nano-scale structural features, which would enhance the accessibility of active sites and molecular transport in the resulting materials [5,20]. Some of these methodologies may be limited by the relatively high cost, the formation of extra-framework aluminium species, partial destruction of the zeolite and irregular mesoporosity resulting from the treatment.[21-22] Hierarchical materials with uniform intracrystalline mesopores based on a number of industrially relevant zeolites, such as FAU, MOR and MFI, have been successfully obtained and utilised for industrial catalysis and separation by means of surfactant-templating post-synthesis modification of zeolites with a wide range of Si/Al ratios using a combination of acid and base treatments in the presence of a surfactant [7,9,23-25]. In addition, hierarchical FAU-type zeolites have been recently prepared in the absence of any organic template, thus offering an affordable route to industrial commercialisation [26-27], compared to procedures making use of costly organic agent [28].

In contrast with the extensive exploitation of mesostructured zeolitic materials in heterogeneous acid-type catalytic processes, their application as basic catalysts has attracted significantly less attention, especially for the transformation of renewable feedstock into valuable chemicals and fuels [5,29-32]. In fact, there have been relatively few attempts aiming to produce basic microporous and mesoporous catalysts. Some of these have been based on the alteration of the chemical compositions of a zeolite, e.g. via ion exchange or impregnation [2,33-34], other approaches utilised more elaborated post-synthesis treatments, such as ammonia grafting [35]. There have been reports focusing on the

application of modified amorphous mesoporous silicas and aluminosilicates (e,g., MCM-41, SBA-15, HMS, etc.), however, these potential catalysts are lacking hydrothermal stability as compared to crystalline zeolites [5,19,35]. Recently, several studies have been carried out aiming to design highly efficient basic catalysts with enhanced access to the active sites inside the zeolite micropores using a network of secondary mesopores. For example, hierarchical FAU and LTA-type zeolites and mesoporous zeolite ETS-10 prepared and tested in Knoevengal condensation of aldehydes as well as for synthesis of α, β-epoxy ketones, have demonstrated a higher catalytic activity as compared to the parent catalysts [36-38]. Parallel to these studies, novel amine-grafted hierarchical zeolites have been successfully synthesised and evaluated as potential catalysts for the aldol condensation of 5-hydroxymethylfurfural [39].

In this work, a range of catalysts based on nanostructured NaY and NaX zeolites have been designed and used for the synthesis of biofuel from vegetable oils using microwave heating. The modification procedures involved two approaches. Firstly, a combination of surfactant mediated acid and base treatments has been utilised aiming to obtain hierarchical faujasites with intracrystalline mesporosity. In the second experiment, the introduction of K and Cs has been carried out via ion-exchange in order to generate more efficient basic catalysts with an enhanced activity in transesterification reactions. The generated mesoporous structure should considerably improve the access by bulky molecules to the zeolite active sites. At the same time, a combination of postsynthetic treatment should not significantly change the Si/Al ratio of the modified faujasites, which should therefore retain their high ion-exchange capacity allowing for the formation of strong basic sites. The aim of the present study is to prepare, characterise and assess faujasite based heterogeneous catalysts with the view to optimise their activity and reaction conditions for the production of biofuel from vegetable oils and to address the importance of the strength of basic sites and their accessibility. The application of microwave heating should allow an increase in the reaction temperature and the reaction rate. A particular emphasis is on the detailed structural characterisation of these nano-structured catalysts in order to evaluate their potential for the transformations of bulky molecules, such as the methanolysis of triglycerides, esterification of free fatty acids and biofuel upgrading reactions.

2. Experimental section

2.1. Materials

The parent zeolites, NaY (CBV-100) and NaX (13X) were obtained from Zeolysts International and Sigma-Aldrich, respectively. Citric acid (99.9%), methanol, n-Hexadecyltrimethylammonium bromide (98%), ethanol, n-heptane and n-hexane (analytical grade, >99.99%), nitric acid (70%), potassium nitrate (99.9%) and potassium hydroxide (86%) were purchased from Fisher Scientific. Refined rapeseed oil, caesium nitrate (99%), caesium hydroxide (99%) and methyl heptadecanoate (analytical GC standard, >99.99%) were supplied by Sigma-Aldrich. Deuterated chloroform (CD_3Cl, 99.8%) and acetonitrile (CD_3CN, 99.8%) were obtained from Cambridge Isotope Laboratories. Pyridine (99.5%, Acros Organics) and pyrrole (99%, Acros Organics) were used as received. Acetylene (99%, BOC) and methyl acetylene (99%, Matheson) were purified in a vacuum system utilising multiple freeze-pump-thaw cycles.

2.2. Preparation of the catalysts

Mesostructured zeolites were prepared according to the method reported in reference [25]. In a typical procedure, 5.0 g of a commercial faujasite was mixed with 50 ml of water and the pH of the slurry was adjusted to ~ 5.5-5.7 using few drops of nitric acid. Then the slurry was stirred with 10% citric acid (using 4.5, 6.0, 9.0 or 12.0 milliequivalents of the acid per 1g of the zeolite) for 1 hour at ambient temperature. After centrifuging and rinsing with deionised water, the acid treated material was recovered and dried for 1 hour at room temperature. The zeolite was re-slurried in a solution containing 0.12-0.75 g of sodium hydroxide and 2.60 g of n-hexadecyltrimethylammonium bromide (CTAB). The mixture was kept at 80-100^{o}C for 24 hour. Next, the solid was recovered, washed and dried in air overnight. To remove the template, 1-3g of the sample was calcined first in the flow of nitrogen at 500^{o}C (temperature ramp of 1.5^{o}C min^{-1}) for 1 hour. Then, the gas flow was switched to oxygen, the temperature was increased to 550^{o}C (temperature ramp of 2^{o}C min^{-1}) and kept for 2 hours before cooling the sample. The obtained mesostructured zeolites were designated as MNaY4.5, MNaY6.0, MNaY9.0, MNaY12.0, MNaX4.5, MNaX6.0, MNaX9.0 and MNaX12.0.

CsNaY, CsNaX, KNaY and KNaX zeolites were produced by adapting methods reported in references [40-41]. The Cs-containing zeolites were prepared by treating the Na-forms with 0.5M of solution containing CsCl and CsOH (4/1 v/v) at 80^{o}C for 1 hour. To produce K-containing zeolites, ion exchange was carried out with 0.5M solution containing KNO_3 and KOH (10/1 v/v) under the same conditions. The exchanged zeolites were washed with deionised water and dried at 80^{o}C overnight.

The same protocol was utilised to obtain CsKNaY and CsKNaX. These catalysts were produced by converting the Na-containing zeolites into their K-forms and then exchanging the latter with the Cs-containing solution.

MNaY6.0 and MNaX9.0 were selected for the ion-exchange modification to produce their Cs- and K-forms. Ion exchange was carried out in two or three steps with 0.1M of solution containing CsCl and CsOH or KNO_3 and KOH (20/1 v/v) at 80^{o}C for 1 hour followed by washing and drying. Four hierarchical zeolites designated as MCsNaY, MKNaY, MCsNaX and MKNaX were obtained using this approach.

Prior to the reaction studies, the catalysts were calcined in a muffle furnace at 450^{o}C for 4 hours (1^{o}C/min temperature ramp) in a flow of oxygen.

2.3. Catalyst characterisation

A detailed structural characterisation of all the catalysts was carried out prior to the reaction studies. Powder X-ray diffraction (XRD) patterns were recorded on a Bruker D8 Advance diffractometer with CuKα radiation at 40kV and 40mA over the 2-theta angle range of 5-60^o. In addition, mesostructured catalysts were characterised in the low 2-theta angle range between 1 and 12^o using 0.3 mm quartz capillaries. The crystalline phases were matched by comparing the XRD patterns of the catalysts with those reported in the literature. The relative crystallinity of hierarchical faujasites was determined from the relative intensities of XRD patterns and their unit cell size was calculated from the XRD data following the ASTM D3906 and ASTM D3942 standard methods; the Si/Al molar ratio and the number of aluminium atoms per unit cell were estimated according to references [42-43].

TM3000 (Hitachi) scanning electronic microscope (SEM) with energy dispersive X-ray analysis (EDX) was utilised to obtain the elemental composition of the catalysts. High-resolution SEM images of mesostructured zeolites were obtained using a PHILIPS XL30 instrument.

The apparent surface areas of the catalysts were calculated using the BET model for the P/P_0 relative nitrogen pressure <0.04; their micro- and mesopore volume and the pore size distribution were computed using the nonlinear density functional theory (NLDFT) model applied to the adsorption branch of the isotherms obtained from the nitrogen adsorption experiments carried out on a Quantachrom Autosorb instrument. The values obtained were scaled to the mass of the activated samples, which was determined by thermogravimetric analysis (TGA) (see Figure S1). The TGA analysis was carried out in flowing nitrogen using a Rheometric Scientific STA 1500 instrument; the sample weight change was measured as a function of temperature (ramped from 20 to 700^{o}C at 10^{o}C/min).

Solid-state NMR experiments were performed using a 400 MHz Bruker Advance III HD spectrometer equipped with a 9.4 T narrow-bore superconducting magnet operating at a Larmor

frequency of 104.26 MHz for ^{27}Al and 79.49 MHz for ^{29}Si. Powdered samples were packed into 2.5 mm rotors and rotated at MAS rates of 15 kHz. NMR spectra were acquired using a pulse-and-acquire pulse sequence, using a relatively short pulse length of 1 μs (radiofrequency field strength of $\gamma B1/2\pi \approx 80$ kHz), and a recycle interval of 0.5 s. Chemical shifts are referenced to 1 M $Al(NO_3)_3$ using a secondary reference sample of Al-ZSM-5 ($\delta = 54$ ppm) for ^{27}Al and to TMS using the cubic octamer Q8M8 ($\delta = -109.8$ ppm) for ^{29}Si.

FTIR spectra were collected using a Thermo iS10 spectrometer in the range 6000-1000 cm^{-1} with the resolution of 4 cm^{-1} and 64 scans in transmission mode. Prior to recording the spectra, the self-supported sample disks (~10 mg/cm^2) were heated in a vacuum cell at 30-450^{o}C (ramp 1^{o}C/min). After a period of 5h at the selected temperature, the sample was cooled to 30^{o}C in vacuum and its IR spectrum was collected. The spectra of adsorbed test-molecules, including pyridine, pyrrole, D_3-acetonitrile and acetylene were obtained at 30^{o}C.

2.4. Composition of rapeseed oil

Rapeseed oil analysed based on density at 15^{o}C (ASTM D4052), the acid value (AV) and the percent FFA were obtained according to American Oil Chemists' Society (AOCS) official methods C-a 5a-40 and C-d 3d-63. 5g of a liquid fat sample was combined with 25 ml of absolute ethanol and few drops of phenolphthalein. The sample then was titrated with 0.1N of KOH. The AV and % FFA were calculated from Equations (1) and (2):

AV (mg KOH/g) = ml of KOH×N of KOH×56.1/ sample mass (g) **(1)**

%FFA= AV×0.503 **(2)**

Fatty acid composition of oil was obtained by gas chromatography-mass spectrometry (GC-MS) according to the official methods ISO 15884 IDF 182:2002(E) and ISO 15885 IDF 184:2002 (E). 100 mg of oil sample was dissolved in 5 ml of n-hexane (Fisher Scientific). The solution then was treated with 200μl of transesterification reagent, 2M methanolic KOH. The mixture was stirred for 5 minutes, then the organic layer was separated and its fatty acid composition was determined by GC-MS using an Agilent 7890A GC with the 5975C mass detection system equipped with a capillary column BPX90 SGE (15m×0.25mm×0.25μm). Each peak in the chromatogram corresponding to FAMEs contents of the parent oil was identified using a NIST library. The GC conditions for this method are shown in Table S1.

The mean molecular weight of the oil (Mwt Oil) was calculated according to the fatty acids in the sample using Equation 3 [44]:

$$\textbf{Mwt Oil} = 3\times \sum(\textbf{Mwt}_i\times\textbf{X}_i) + 38 \quad (3)$$

Where MW_i and X_i stand for the molecular weight and the fraction of the fatty acids in the oil.

2.5. Methanolysis of rapeseed oil

The reaction studies were carried out in a Biotage microwave system (Biotage Initiator+). Specially designed 20-ml glass vials were used at elevated temperature and pressures (up to 160^{o}C and 15 bar). In a typical transesterification reaction run, 10 ml of rapeseed oil was reacted with methanol at a 1:9, 1:12 or 1:18 molar ratio at 160^{o}C for 1-11 hours with continuous automated stirring using 5, 10 or 20 wt% of the catalyst (relative to the amount of rapeseed oil).

At the end of reaction, the mixture was centrifuged and the upper layer contained FAMEs and methanol was separated. The excess methanol was removed using a rotary evaporator and the FAMEs were analysed to determine the reaction yield and selectivity.

2.6. Stability and reusability of catalysts

Following the transesterification reaction, the catalyst was separated, washed with methanol 3 times and dried overnight at 60^{o}C. The dried zeolite was calcined under the same conditions as prior to the initial reaction and utilised again in the transesterification of rapeseed oil. The same reaction conditions were used in the consecutive runs for the recycled catalyst.

2.7. Analysis of the reaction products

FAMEs were characterised by FTIR, using a Thermo iS10 spectrometer in the range 4000-400 cm^{-1} with the resolution of 4 cm^{-1} and 64 scans. The position of stretching and bending vibrations in the spectra of biodiesel and parent oil were compared to the literature data [45]. The ester groups were identified by the C=O absorption bands around 1760-1730 cm^{-1} and the C-O band between 1300 and 1100 cm^{-1}.

^{1}H-NMR spectroscopy (Bruker Advance 300 spectrometer) was applied as an efficient tool to determine the yield of the transesterification reaction using D-chloroform ($CDCl_3$) as a solvent for this procedure. The conversion of oil to FAMEs was calculated using Equation 4 [46:]

$$\textbf{Conversion (\%)} = 100 \times (2\textbf{I}_{\textbf{Me}}/3\textbf{I}_{\textbf{CH2}}) \quad (4)$$

Where I_{Me} is the integrated area of the methoxy group protons at 3.60 ppm, and I_{CH2} represents the integrated area of the methylene group protons at 2.30 ppm. At the same time, the purity of FAMEs was confirmed by the disappearance of the glycerol-related signal at 4.1-4.4 ppm.

The ester content of fatty acid methyl esters in biofuel was also determined according to the standard test method EN-14103. The internal standard solution of methylheptadecanoate was prepared with concentration of 10 mg/mL in n-heptane. 0.1 ml of the purified reaction products was dissolved in 2 ml of the internal standard solution and then injected in to the Agilent 6890 GC equipped with an FID and the same column that was used in the characterisation of oils (see Table S2). The peak area for the ester components of the FAME C14:0 to C24:1 was used to calculate their mass fraction in percent (see Equation 5 and Figure S1):

$$\mathbf{C = (\sum A - AEI) / AEI \times (CEI \times VEI / m) \times 100\%} \quad \mathbf{(5)}$$

Where C is the ester content in percent, ∑A is the total peak area from C14:0 to C24:1, AEI is the peak area of internal standard solution, CEI is the concentration of internal standard solution in mg/ml, VEI is the volume of internal standard solution in ml and m is the mass of sample in mg.

3. Results and discussion

3.1. Characterisation of mesostructured faujasites

Two series of catalysts based on modified zeolites NaX and NaY have been characterised in this work using a range of techniques in order to evaluate their structural features such as crystallinity, chemical composition, porosity and the presence of basic sites.

Figure S2 shows the XRD patterns of mesostructured faujasites prepared via a two-step combination of acidic and basic treatments. For both NaY and NaX zeolites, as the amount of citric acid used in the first step increases the peak intensity in the patterns decreases, reflecting the degree of structural degradation, which can be explained by the cleavage of the Al-O bonds in the presence of the acid [9]. This becomes particularly significant as the amount of citric acid exceeds 6 meq/g of zeolite; indeed, samples MNaY12.0 and MNaX12.0 are amorphous.

The two-step acid-base treatment has been carefully monitored in this work targeting controlled consecutive dealumination and desilication of the faujasite structure. At the same time, the presence of the CTAB surfactant facilitates an "orderly" partial destruction of the zeolite framework with the formation of a bimodal pore system comprising the original faujasite micropores and secondary mesopores with the diameter matching that of the CTAB micelles. Table 1 and Figure S3 summarise the structural properties of the prepared hierarchical zeolites. The data demonstrate that achieving successful modification of these materials is associated with careful control of citric acid addition up to 9.0 meq/g, which prevents severe dealumination and degradation of the crystalline structure. It

appears that during the following mild treatment under basic conditions, the surfactant is protecting the Si-O-Si and Si-O-Al bonds from excessive cleavage, resulting in the formation of a hierarchical pore system within the faujasite structure. In agreement with previous reports, the amount of citric acid utilised during the post-synthesis modification of faujasites can control the degree of mesoporosity [9]. Indeed, the micropore volume is decreasing whilst the mesopore volume is increasing with the amount of citric acid used for both NaY and NaX zeolites (Figure S3). Furthermore, the comparison of Si/Al ratios obtained from the SEM-EDX (accounts for the total Al and Si content) and XRD (takes into account only Si and Al in the framework) indicates that the prepared mesostructured zeolites (especially "over-treated" samples, e.g. MNaY9.0 and MNaY12.0) contain some "extra-framework silicon", e.g. clusters of amorphous silica, rather than extra-framework aluminium - this is also confirmed by our NMR and FTIR data (see below).

Nitrogen adsorption data (Figure 1) demonstrate remarkably different isotherm profiles for the parent faujasites (type I) and the modified materials (type IV). In particular, MNaY6.0 sample displays the H4 type hysteresis loop commonly found in mesoporous zeolites [47], which is consistent with the bimodal pore size distribution showing the presence of both micro- and mesopores (Figure 1b). The step-down feature observed for the desorption branch of the hysteresis loop is associated with cavitation induced evaporation from mesopores. As recently reported in references 25 and 47, a detailed analysis of connectivity between micropores and mesopores in hierarchical Y-type zeolites carried out combining argon and nitrogen adsorption at different temperatures with hysteresis scanning has demonstrated the presence of interconnected intracrystalline micro- and mesopores in these systems. Although our work is not focused on the mechanism by which the intracrystalline mesoporosity in faujasites is generated, a significant insight into this process can be gained from the results obtained on very similar systems, which have been reported by Garcia-Martinez et al.[25] Their TEM data clearly demonstrate that in the case of NaY zeolite, the combination of carefully executed acid and base treatments in the presence of a surfactant leads to the formation of a catalyst with regular intracrystalline mesopores, rather than a composite material comprising of the microporous zeolite and amorphous mesoporous silica.[25] An indirect confirmation of this conclusion comes from our FTIR data obtained for the back-exchanged ammonium forms of NaY and MNaY6.0 zeolites following their activation at 450^{o}C and pyridine adsorption at 150^{o}C (see Figure S4). The spectra indicate that the accessibility of acid sites in D6R and sodalite cages is significantly greater for the MNaY6.0 based sample, which would not be expected if it was a composite material.

Table 1. Properties of the mesostructured faujasite-type zeolites.

Zeolite	Si/Al (SEM)	Si/Al (XRD)	Al_{uc}	UCS (Å)	Crystallinity %	S_{BET} (m^2g^{-1})
NaY	2.5	2.5	54	24.66	99	855
MNaY4.5	3.0	2.8	50	24.63	73	770
MNaY6.0	4.0	3.2	46	24.59	65	830
MNaY9.0	4.5	3.3	45	24.57	42	605
MNaY12.0	13.0	-	-	-	0	580
NaX	1.2	1.1	92	24.97	100	910
MNaX4.5	1.4	1.2	90	24.94	79	655
MNaX6.0	1.4	1.3	82	24.91	56	600
MNaX9.0	1.8	1.5	77	24.85	31	510
MNaX12.0	2.4	-	-	-	0	340

Notes: Al_{uc} is the number of Al atoms per unit cell, UCS is unit cell size; S_{BET} is the BET apparent surface area.

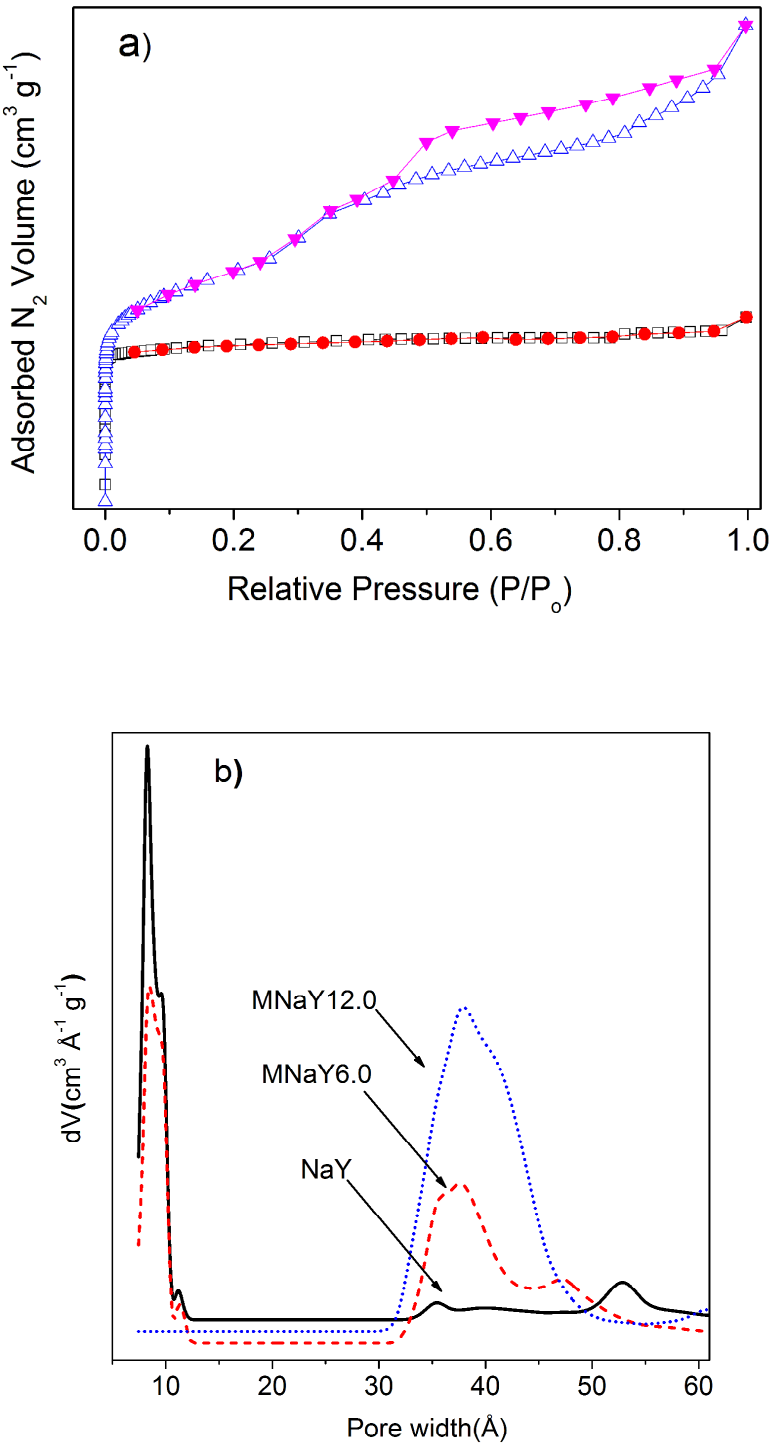

Figure 1. N_2 adsorption isotherm of (a) hierarchical zeolite MNaY6.0 - blue trianges and parent NaY – black squares; (b) pore size distribution for NaY, MNaY6.0 and MNaY12.0. (Filled symbols correspond to the nitrogen desorption data.)

The "over-treated" amorphous MNaY12.0 material, whilst still having a very high surface area and pore volume, shows a monomodal pore size distribution similar to that of MCM-41 type materials, confirming that the microporous zeolite structure has collapsed. Interestingly, the mesopores present in both MNAY6.0 and MNaY12.0 samples have a significant degree of the long-range order as revealed by the low-angle XRD data (see Figure 2) with the peaks found at 2.5° for the mesostructured zeolite MNAY6.0 (d-spacing ~3.46 nm) and at 2.1° for the amorphous MNaY12.0 material (d-spacing ~4.03nm).

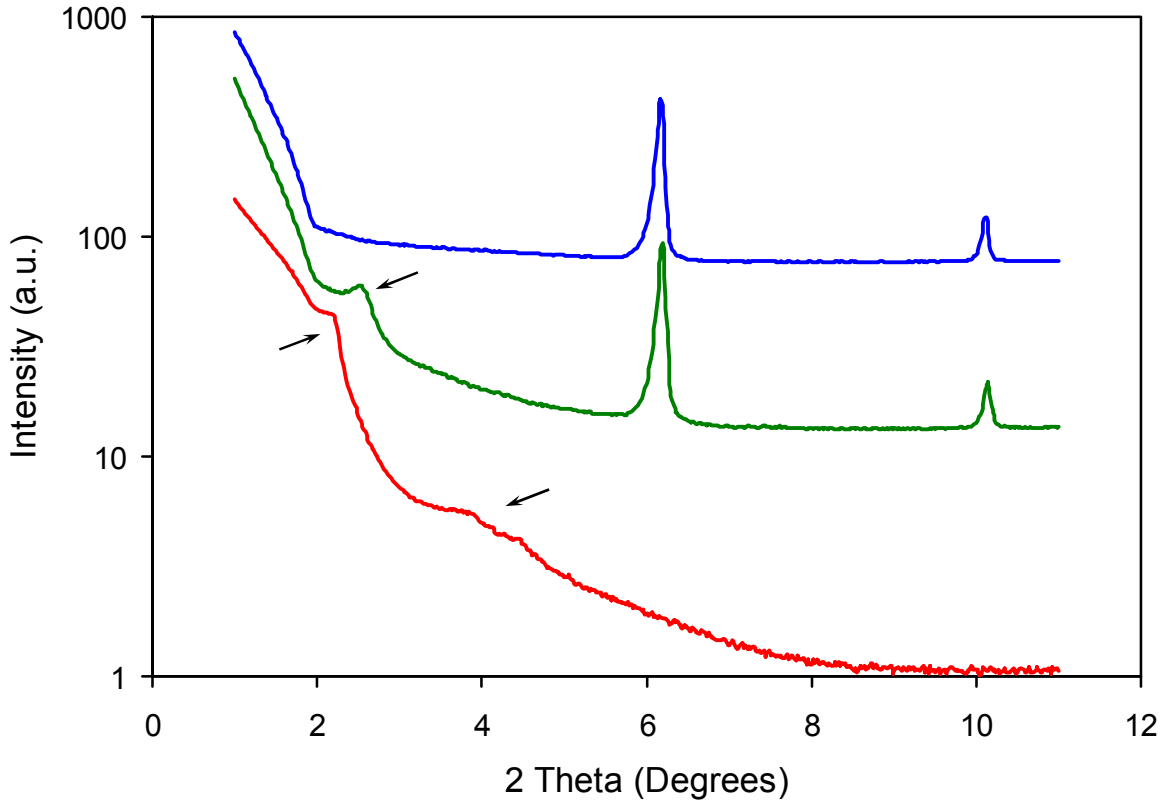

Figure 2. Low-angle XRD patterns of (top to bottom) parent zeolite MNaY6.0 zeolite and MNaY12.0 sample.

The SEM images of the hierarchical MNAY6.0 faujasite (Figures 3 and S5) also reveal the presence of secondary mesopores as well as some macropores and the sponge-like structure of zeolite particles.

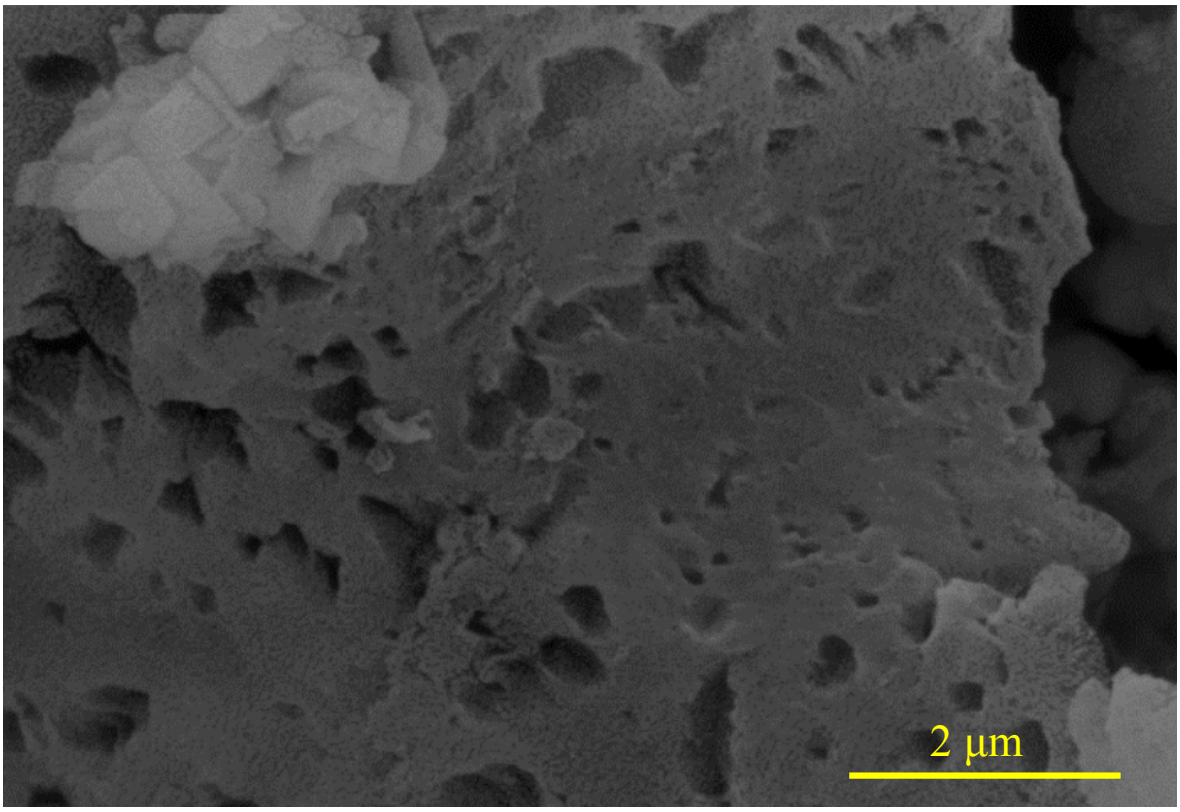

Figure 3. SEM image of the of hierarchical MNaY6.0 zeolite.

In general, zeolites treated with either an acid or a base can contain significant amounts of extra-framework aluminium [48]. Our ^{27}Al MAS NMR data (Figure 4), in agreements with the previous study [9], show no extra-framework Al signal at 0 ppm, which would correspond to the typical chemical shift of the six-coordinate Al. The only aluminium signal that is observed in the ^{27}Al MAS NMR spectra is that of tetrahedrally coordinated species, which are typically found between 40-65 ppm [49]. The tetrahedral Al peak becomes asymmetric for the samples treated with increasing amount of citric acid. The 2D data (Figure S6) indicate that the disorder in the four-coordinate Al species is coming primarily from chemical shift dispersion and not the change in the quadrupole coupling interaction, that is the four-coordinate species are affected by the changes in the chemical environment (e.g. the number of Al and Si atoms in the second coordination sphere), but the local coordination sphere appears to remain constant. ^{29}Si MAS NMR spectra indicate a moderate increase in the framework Si/Al ratio as the amount of citric acid utilised in the faujasite modification is increasing (Figure 5). It should be noted that although ^{29}Si MAS NMR spectra can be utilised to compute the framework Si/Al ratio in dealuminated faujasite, such calculations become at best semi-quantitative if the zeolite modification is accompanied with a significant increase in the number of terminal Si-OH groups, which would affect the intensity of the Q^0-Q^3 signals; such silanols have been observed in the FTIR spectra of all mesoporous faujasites (see Figure 6).

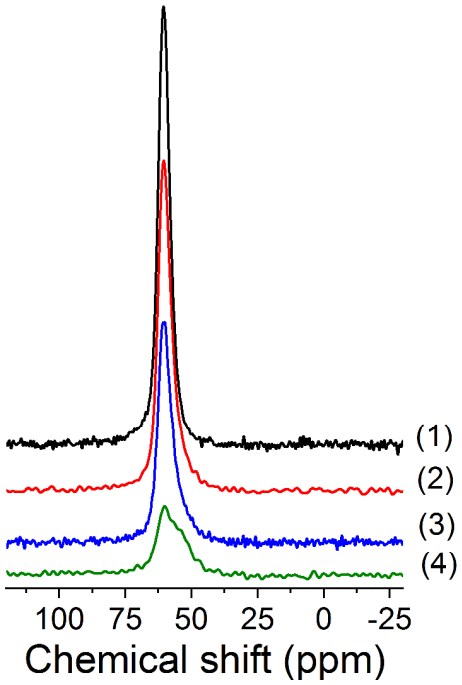

Figure 4. ^{27}Al (9.4 T, 15 kHz) MAS NMR spectra of NaY with different dosage of citric acid. (1) - NaY; (2) - MNaY4.5; (3) - MNaY6.0; (4) - MNaY9.0.

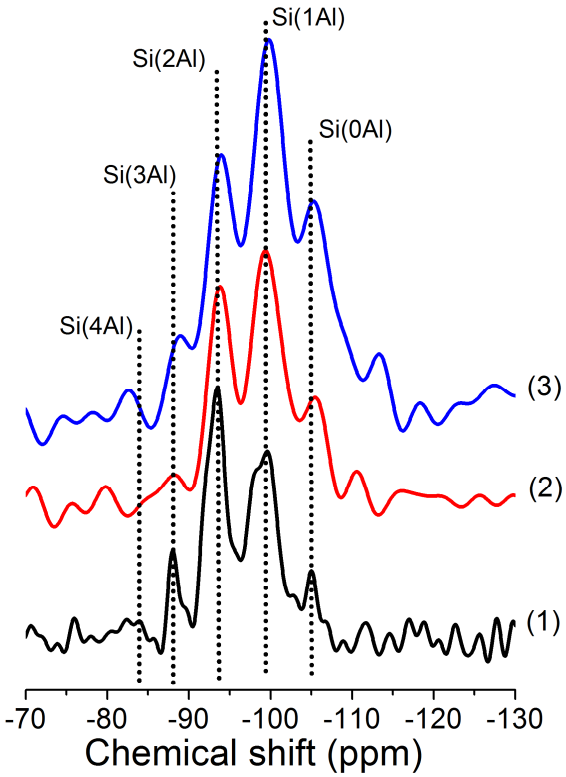

Figure 5. ^{29}Si MAS NMR spectra of NaY samples treated with increasing dosage of citric acid (1) - NaY; (2) - MNaY4.5; (3) - MNaY6.0.

The FTIR spectra of the parent and modified NaY zeolites before and after Py adsorption are presented in Figure 6. The parent NaY has almost no OH-groups, which is indicative of a material with very few defects or impurities. The major peak at 1444 cm^{-1} for this sample is attributed to Py molecules interacting with Na^{+} cations, at the same time, no peaks due to Py complexes with Brønstead or Lewis acid sites (BAS and LAS) have been detected. As the pretreatment conditions become more severe, a band at 3745 cm^{-1} with increasing intensity is observed in the OH region, this is assigned to Si-OH groups. At the same time, the intensity of the Py--Na^{+} peak decreases and a low intensity peak due to Py--LAS complexes appears at 1454 cm^{-1}. This can be explained by the formation of amorphous silica clusters and Si-OH defect sites in the zeolite structure during both the dealumination and desilication procedures. The very low level of the LAS, generally associated with extra-framework Al species, suggests that most frameworks Al dislodged during the acid treatment is chelated by the citric acid and removed from the system.

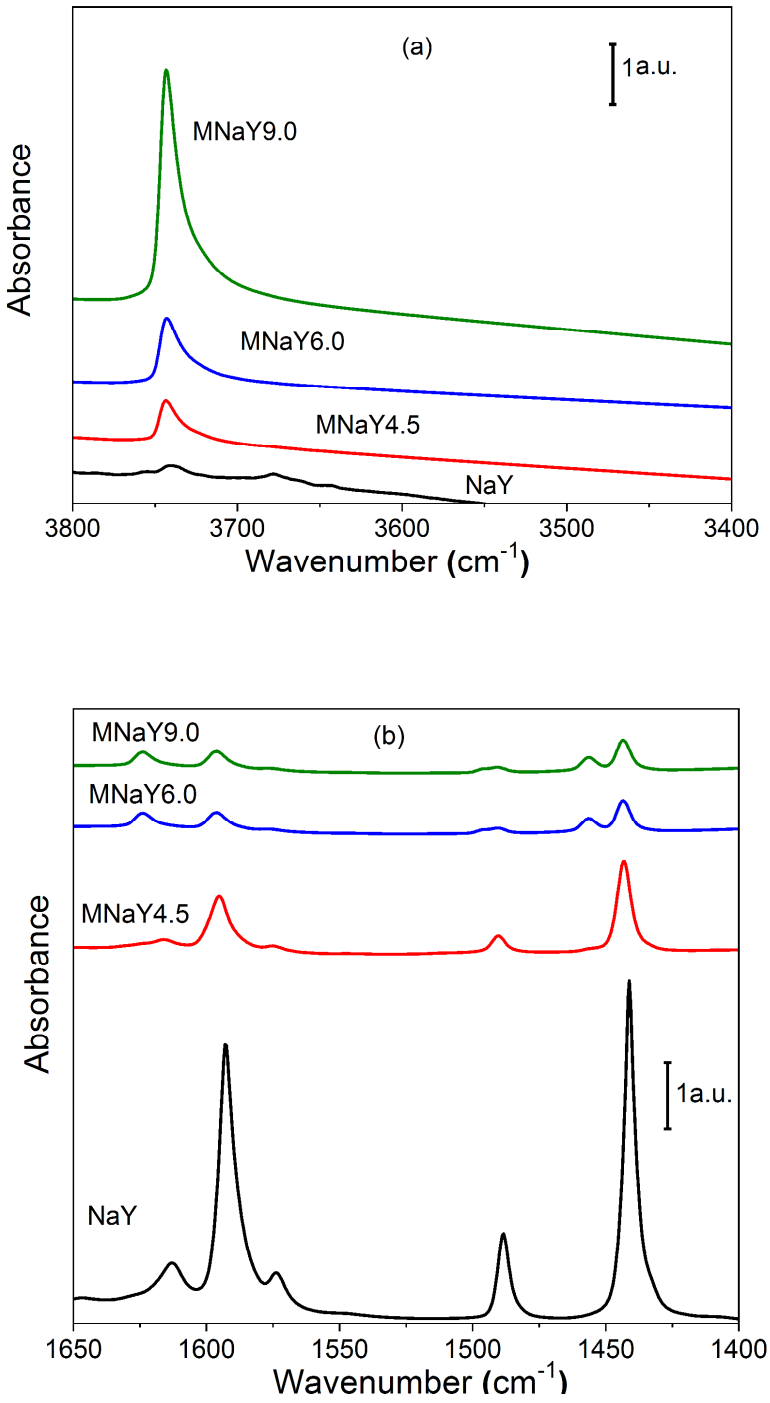

Figure 6. FTIR spectra of mesostructured Y zeolites: (a) - the OH region of samples activated at 450°C and (b) - Py region following Py adsorption on the activated samples.

3.2. Characterisation of ion-exchanged faujasites

The parent NaY and NaX zeolites and some of the mesostructured faujasites have been ion-exchanged with K and Cs cations in order to enhance their basic character making them more active catalysts in rapeseed oil transesterification [50]. The XRD patterns of the cation-exchanged parent zeolites are shown in Figures S5 and S6. In agreement with previous findings, the data confirm the high crystallinity of these materials [51]. Chemical analysis and nitrogen adsorption data for modified faujasites are summarised in Table S3. The exchange of Na cations for K and Cs has been also confirmed by FTIR of adsorbed test molecules, such as Py and CD_3CN. In general, the extent of ion-exchange for K than Cs cations is limited as these species are too large to readily access cation positions in sodalite cages and D6R units of the faujasite structure. The relatively high degree of ion-exchange achieved for CsKNaY and CsKNaX samples following multiple exchanges with both K and Cs could be explained by the partial degradation of the faujasite structure during these procedures, which may lead to a greater accessibility of the cationic positions in smaller cages. In addition, some degree of "over-exchange", as reported by Busca [2], cannot be ruled out. The larger space occupied by the Cs cations and partial structural degradation can explain the decrease in the apparent surface area and pore volume in Cs-exchanged zeolites as measured by nitrogen adsorption.

The basic sites of the prepared catalysts have been characterised by the adsorption of pyrrole and acetylene as probe molecules monitored by FTIR. The changes in the N-H vibrational frequency as pyrrole forms a hydrogen bond with oxygen atoms of the catalyst can be used as an indication of its basicity [52-54]. Figure S8 shows a clear trend - with the decreasing Si/Al ratio and increasing degree of Na substitution by K and Cs, the broad band N-H vibration is shifting to low frequency, thus confirming the greater basic character of zeolite X as compared to zeolite Y, and of K- and Cs-faujasites as compared to their Na-forms. This is consistent with the FTIR data obtained using acetylene. For NaX, a high intensity peak of the C-H stretching vibration is observed at 3187 cm^{-1} representing a 100 cm^{-1} shift as compared to the gas phase value for acetylene of 3287 cm^{-1}, which is due to acetylene molecules interacting with basic oxygen atoms with the formation of a hydrogen bond [55] . Slightly more basic oxygen sites are detected in KNaX and CsKNaX, the C-H stretching vibration at 3190 cm^{-1}, whereas Na-, K- and Cs-forms of zeolite Y are less basic compared to their zeolite X counterparts.

3.3. Composition of rapeseed oil

Table S4 shows the results of rapeseed oil analysis. The composition of the oil has been confirmed based on specific retention times in the chromatogram and characteristic fragmentation pattern in the

mass spectra. The major fatty acid component at 77% in rapeseed oil is oleic acid, C18:1. The data also indicate that the oil contains a small amount of FFA, which according to the literature shows little or no effect on the catalytic activity of the solid catalysts.

3.4. Transesterification reaction

To investigate the activity of basic faujasite catalysts in transesterification of rapeseed oil, a series of experiments has been conducted using a batch type reactor under conventional and microwave heating. The reaction products have been monitored by ^{1}H NMR, GC-MS and FTIR (see Figures S9, S10 and S11). For example, characteristic signals have been identified in biodiesel using chemical shifts in ^{1}H NMR (3.60 ppm for -OCH_3 and 2.30 ppm for -CH_2). Microwave heating can greatly enhance the reaction rate, and the highest conversion (~90% for CsKNaX zeolite) has been observed in this work within a shorter period using the highest temperature achievable with the Biotage microwave equipment (160^{o}C for the methanol based reaction systems). Our results demonstrate significantly shortened reaction times as compared to the literature [56], which reports the highest yield (over 90% conversion, ~100% selectivity) obtained in the conventional heating mode after 7 hours using K_2O/NaX as basic heterogeneous catalyst. The significant acceleration of the transesterification reaction has been explained by the higher temperatures that are achieved using microwave irradiation in comparison to the conventional or supercritical systems, which is due to the high polarity and hence high microwave absorption ability of methanol [57-58]. Although there is a significant difference in microwave absorption by methanol and the oil, the reaction selectivity for all catalysts is close to 100% and no unusual patterns in the product distribution have been observed as compared to the systems utilising conventional heating.

The following experiments have been carried out in the Biotage microwave system aiming to evaluate the role of the sample calcination, molar ratio between the oil and methanol, catalyst to oil ratio and the reaction duration. The effect of sample calcination at 450^{o}C, prior to the catalyst loading into the batch reactor, has been examined for K and Cs exchanged faujasites. The results show an ~4-fold activity enhancement for the zeolites calcined ex situ before the reaction run. Hence, all the reaction data presented below have been obtained for the calcined catalysts. In agreement with the previous reports, our data demonstrate (Figure S12) that the conversion of rapeseed oil is increasing with the amount of catalyst utilised in the batch reactor reaching a plateau at around 10wt% of the catalyst [59-60].

The effect of the oil to methanol molar ratio on the triglyceride conversion is shown in Figure 7. Our results confirm that conversion increases for systems with a higher molar ratio, which has been

explained by the reduced mass transfer limitations due to the immiscibility of the oil and alcohol [61]. It should be noted that previous reports suggest that the molar ratios between 1:6 and 1:275 can be utilised to obtain high yield of biodiesel within 24 hours [59-60].

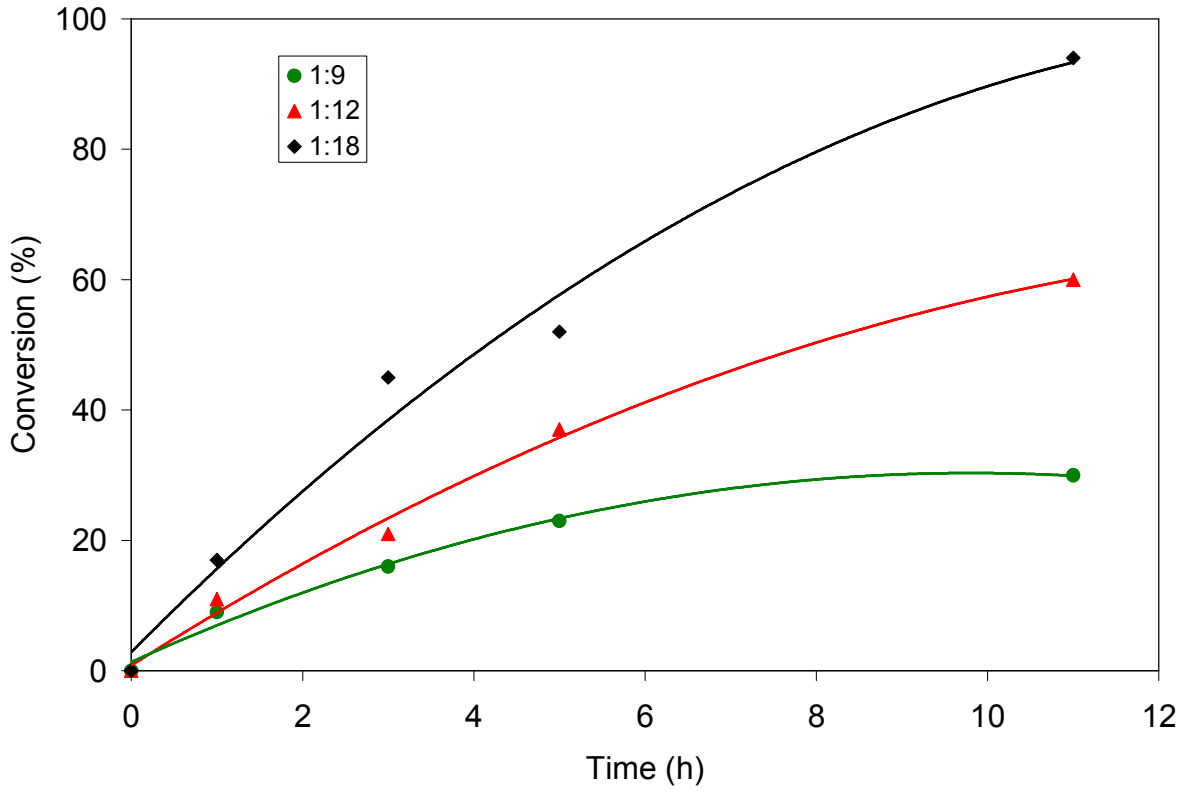

Figure 7. The effect of the oil to methanol molar ratio on transesterification of oil using CsNaX.

Table S5 presents a comparison of the rapeseed oil conversion data obtained on ion-exchanged faujasites, which demonstrate two clear trends: (i) zeolite X based catalysts are more active than those based on zeolite Y and (ii) the activity of these zeolites increases with the degree of ion-exchange with more electropositive cations. Both trends coincide with the strength of the basic sites in the alkali-exchanged faujasites associated with the framework oxygen atoms [33]. Indeed, zeolites NaX and KNaX have stronger basic sites than related NaY and KNaY zeolites, the former achieving a higher yield of FAMEs, 29 and 86% respectively, whereas the latter show the yield of 8 and 73% only. In order to increase the basic character of these zeolites, two catalysts have been prepared via successive exchanges with K and Cs cations. CsKNaX exhibited a significantly higher activity in the transesterification reaction reaching up to 90% conversion within 1 hour of the reaction time and a relatively low concentration of methanol (Table 2). These findings are in agreement with the conclusions of previous reports [2,33] that the strength of basic sites on alkali metal exchanged zeolites

increases with increasing Al content, their ion-exchange capacity and with the presence of more electropositive cations in the sequence Li<Na<K<Rb<Cs, all of which enhance the mean negative charge on the oxygen atoms of the zeolite framework. Structural stability, high surface area and strong bonding with the active phase preventing the loss of the active sites during the reaction and regeneration cycle are essential characteristics of the catalysts utilised in the production of biodiesel. Indeed, many basic catalysts produced via impregnation of alkali hydroxides and carbonates are known to suffer from the leaching of the active component during the reaction and regeneration cycles [56]. Zeolites prepared and tested in this work have been generated via ion-exchange rather than impregnation, and our data indicate little, if any, occlusion of alkali oxide or hydroxide in the ion-exchanged materials. These catalysts have shown no leaching of K or Cs and have retained their high activity in several consecutive runs.

Table 2. Transesterification of rapeseed oil with methanol: comparison of K- and CsK- forms of basic faujasites.

Catalysts	Run	Catalysts amount (wt %)	Oil:methanol molar ratio	Reaction time (h)	Conversion (%)	Selectivity (%)
KNaX	1	10	1:18	1	30	>99
CsKNaX	1	5	1:9	1	58	>99
			1:12	1	90	>99
KNaY	1	10	1:18	1	30	>99
CsKNaY	1	5	1:9	1	38	>99
			1:12	1	50	>99

The results of transesterification reaction studies on basic hierarchical faujasites are presented in Table S5. Their catalytic activity is found to decline with decreasing framework aluminium content in the zeolites, thus demonstrating that the strength of the basic sites plays a greater role in this reaction than the more open structure of the catalysts, and hence, limiting their potential as basic catalysts. Several recent studies [36-39] reported the application of nano-structured zeolites for liquid phase transformations of organic compounds. For instance, Perez-Ramirez et al.[36] conducted condensation of benzaldehyde with malononitrile over basic hierarchical zeolites demonstrating that the catalyst activity increases with increased mesoporosity and improved access to active sites as this reaction involves transformation of bulky molecules. It should be noted that Knoevenagel

condensation does not need a very strong base as a catalyst since the pK_a of malononitrile is ~11. In contrast, transesterification of triglycerides requires a more basic catalyst as the pK_a of methanol is ~15.5. This is consistent with a recent communication [39] indicating that both accessibility of the porous structure of hierarchical zeolites and the presence of basic sites are important in aldol condensation. The influence of each of these factors may differ depending on the reaction type and conditions. Indeed, our preliminary data indicate that basic small-pore zeolites, such as K-form of LTA, are more active in the methanolysis of triglycerides than K-forms of faujasites, although the pore size of the former would preclude the access of most organic molecules to the micropores.

4. Conclusion

The application of heterogeneous catalysts in the production of biofuel offers potential advantages including lower cost, high stability and the ease of separation. Recent progress in the synthesis of novel zeolite structures and methodologies for their modification stimulated new developments in many areas, including catalysis, separation and sensor applications. For instance, hierarchical zeolites with a bimodal pore size distribution provided a viable solution for enhancing active site accessibility and reducing the mass transfer problems in heterogeneously catalysed reactions. A combination of post-synthesis modifications of faujasites, including ion-exchange with Cs^+ and K^+ and successive acid and base treatments accompanied with surfactant templating, was applied in this work in order to obtain basic cation-rich zeolites X and Y with intracrystalline systems of secondary mesopores as potential catalysts for biofuel production. The prepared hierarchical zeolites were characterised by XRD, SEM, nitrogen adsorption, FTIR, solid state NMR and tested in the transesterification of rapeseed oil. The reaction studies were performed under microwave heating and the effects of the reaction conditions, basic properties and pore structure of the modified faujasites were evaluated. The conversion of triglycerides increased with increasing Al content and concentration of Cs and K in modified zeolites. In particular, CsKNaX exhibited the highest activity in the transesterification reaction achieving 90% conversion within 1 hour of the reaction time, thus confirming that the strength of basic sites in zeolites is enhanced by the increasing amount of Al, their ion-exchange capacity and by the presence of more electropositive cations, such as K and Cs. The activity of hierarchical X and Y zeolites declined as their framework Si/Al ratio increased. Although nitrogen adsorption and FTIR data clearly show that the mesostructured faujasites have a more open pore structure, and therefore, their activity should be less affected by the mass transfer limitations, even a modest increase in the Si/Al ratio of the modified zeolites results in a lower ion-exchange capacity and a lower negative charge on the oxygen atoms. As a consequence, the cationic

forms of both mesostructured X and Y zeolites are weaker bases than their microporous counterparts, which is confirmed by both spectroscopic and catalytic studies. Overall, this work demonstrates that the strength rather than accessibility of basic sites in cationic forms of modified faujasites determines the catalytic performance of these nanostructured materials in transesterification of triglycerides. Clearly, the balance between the strength of the active sites and their accessibility in X and Y zeolites would have to be fine-tuned for different applications. For instance, our preliminary results indicate that nano-structured faujasites converted into their acidic forms are highly effective in esterification of free fatty acids. Indeed, such materials employed in acid-catalysed transformations of bulky molecules should demonstrate the full potential of the enhanced accessibility of active sites.

Supporting information available: details of the reaction products analysis; additional XRD, SEM, NMR, FTIR, TGA and catalytic data.

Conflict of interest

The authors declare no conflict interest.

Acknowledgments

This work was supported by Oil Marketing Company (SOMO), Baghdad, Iraq under grant SL-144-02. The authors appreciate the support of the Lennard-Jones Laboratories at Keele University, UK, where this study was carried out. The authors thank Dr.Kunhao Li of Rive Technology, USA, for his advice and support.

5. References

(1) Ennaert, T.; Van Aelst, J.; Dijkmans, J.; De Clercq, R.; Schutyser, W.; Dusselier, M.; Verboekend, D.; Sels, B.F. Synthesis, Characterisation, and Catalytic Evaluation of Hierarchical Faujasite Zeolites: Milestones, Challenges, and Future Directions. *Chemical Society Reviews*. **2016**, *45*, 3331-3352.

(2) Busca, G. Acidity and Basicity of Zeolites: A Fundamental Approach. *Microporous and Mesoporous Materials*.**2017**, *254, 3*-16.

(3) Martínez, C.; Corma, A. Inorganic Molecular Sieves: Preparation, Modification and Industrial Application in Catalytic Processes. *Coordination Chemistry Reviews*. **2011**, *255*, 1558-1580.

(4) Primo, A.; and Hermenegildo G. Zeolites as Catalysts in Oil Refining. *Chemical Society Reviews*. **2014**, *43*, 7548-7561.

(5) Davis, M. E. ,Mesoporous Zeolites: Preparation, Characterization and Applications, ed García-Martínez, J. ; and Li,K. *John Wiley & Sons*, **2015**.

(6) Schwieger, W.; Machoke, A. G.; Weissenberger, T.; Inayat, A.; Selvam, T.; Klumpp, M.; Inayat, A. Hierarchy Concepts: Classification and Preparation Strategies for Zeolite Containing Materials with Hierarchical Porosity. *Chemical Society Reviews*.**2016**, *45*, 3353-3376.

(7) Li, K.;Valla, J.;Garcia‐Martinez, J. Realizing the Commercial Potential of Hierarchical Zeolites: New Opportunities in Catalytic Cracking. *Chem. Cat. Chem.* **2014**, 6, 46-66

(8) Koohsaryan, E.; Anbia, M. Nanosized and Hierarchical Zeolites: A Short Review. *Chinese Journal of Catalysis*. **2016**, *37*, 447-467.

(9) García-Martínez, J.;Johnson, M.; Valla, J.; Li, K.; Ying, J.Y. Mesostructured Zeolite Y—high Hydrothermal Stability and Superior FCC Catalytic Performance. *Catalysis Science & Technology*. **2012**, *2*, 987-994.

(10). Chal, R.; Gerardin, C.; Bulut, M.; van Donk, S. Overview and Industrial Assessment of Synthesis Strategies Towards Zeolites with Mesopores. *ChemCatChem*.**2011**, *3*, 67-81

(11) Pérez-Ramírez, J.; Christensen, C. H.; Egeblad, K.; Christensen, C. H.; Groen, J. C. Hierarchical Zeolites: Enhanced Utilisation of Microporous Crystals in Catalysis by Advances in Materials Design. *Chemical Society Reviews* .**2008**, *37*, 2530-42.

(12) Egeblad, K.; Christensen, C. H.; Kustova, M.; Christensen, C. H. Templating Mesoporous Zeolites. *Chemistry of Materials*. **2007**, *20*, 946-960.

(13) Lopez-Orozco, S.; Inayat, A.; Schwab, A.; Selvam, T.; Schwieger,W. Zeolitic Materials with Hierarchical Porous Structures. *Advanced Materials*. **2011**, *23*, 2602−2615.

(14) Linares,N.;Silvestre-Albero,A.M.;Serrano,E.;Silvestre-Albero,J.;García-Martínez,J.Mesoporous Materials for Clean Energy Technologies. *Chemical Society Reviews*. **2014**, *43*, 7681-7717.

(15) Jiyang, L.i.; Corma, A.; and Yu J. Synthesis of New Zeolite Structures. *Chemical Society Reviews*, **2015**, *44*, 7112-7127.

(16) Liu, Z.; Hua, Y.; Wang, J.; Dong, X.; Tian, Q.; Han, Y. Recent Progress in the Direct Synthesis of Hierarchical Zeolites: Synthetic Strategies and Characterization Methods. *Materials Chemistry Frontiers*. **2017**, *1*, 2195-2212.

(17) Pérez-Ramírez, J. Zeolite Nanosystems: Imagination Has No Limits. *Nature Chemistry*.**2012**, *4*, 250-251.

(18) Serrano, D.P.; and Pizarro, P.; Escola, J.M. Synthesis Strategies in the Search for Hierarchical Zeolites. *Chemical Society Reviews*.**2013**, *42*, 4004-4035.

(19) Prasomsri, T.; Jiao, W.; Weng, S. Z.; Garcia Martinez, J. Mesostructured Zeolites: Bridging the Gap between Zeolites and MCM-41.*Chemical Communications*.**2015**, *51*, 8900-8911.

(20) Hartmann, M.; Machoke, A. G.;; Schwieger, W. Catalytic Test Reactions for the Evaluation of Hierarchical Zeolites. *Chemical Society Reviews*. **2016**,*45*, 3313-3330.

(21) Silaghi, M.-C.; Chizallet, C.; Raybaud, P. Challenges on Molecular Aspects of Dealumination and Desilication of Zeolites. *Microporous and Mesoporous Materials*. **2014**,*191*, 82-96.

(22) Losch, P.; Hoff, T. C.; Kolb, J. F.; Bernardon, C.; Tessonnier, J.-P.; Louis, B. Mesoporous ZSM-5 Zeolites in Acid Catalysis: Top-Down Vs. Bottom-Up Approach. *Catalysts* .**2017**,*7,* 225.

(23) Valtchev, V.; Majano, G.; Mintova, S.; Pérez-Ramírez, J. Tailored Crystalline Microporous Materials by Post-Synthesis Modification. *Chemical Society Reviews*. **2013**,*42*, 263-90.

(24) Verboekend, D.; Vilé, G.; Pérez‐Ramírez, J. Hierarchical Y and USY Zeolites Designed by post‐synthetic Strategies. *Advanced Functional Materials*. **2012**, 22, 916-928.

(25) Sachse, A.; Grau-Atienza, A.; Jardim, E.O.; Linares, N.; Thommes, M.; Garcia-Martinez, J Development of Intracrystalline Mesoporosity in Zeolites through Surfactant-Templating. *Crystal Growth & Design.* **2017**, *17*, 4289-4305.

(26) Inayat, A.; Schneider, C.; Schwieger, W. Organic-Free Synthesis of Layer-Like FAU-Type Zeolites. *Chemical Communications* .**2015**, *51*, 279-281.

(27) Ferdov, S. FAU-Type Zeolite Nanosheets from Additives-Free System. *Microporous and Mesoporous Materials*.**2017**, *242*, 59-62.

(28) Inayat, A.; Knoke, I.; Spiecker, E.; Schwieger, W. Assemblies of Mesoporous FAU‐Type Zeolite Nanosheets. *Angewandte Chemie International Edition*. **2012**, 51, 1962-1965.

(29) Shanbhag, G. V.; Choi, M.; Kim, J.; Ryoo, R. Mesoporous Sodalite: A Novel, Stable Solid Catalyst for Base-Catalyzed Organic Transformations. *Journal of Catalysis*. **2009**,*264*, 88-92.

(30) Weitkamp, J.; Hunger, M.; Rymsa, U., Base Catalysis on Microporous and Mesoporous Materials: Recent Progress and Perspectives. *Microporous and Mesoporous Materials*. **2001**,*48*, 255-270.

(31) Perego, C.; Bosetti, A.; Ricci, M.; Millini, R. Zeolite Materials for Biomass Conversion to Biofuel. *Energy & Fuels.* **2017**, *31*, 7721-7733.

(32) Serrano, D. P.; Melero, J. A.; Morales, G.; Iglesias, J.; Pizarro, P. Progress in the Design of Zeolite Catalysts for Biomass Conversion into Biofuels and Bio-Based Chemicals. *Catalysis Reviews*. **2017**, 1-70.

(33) Barthomeuf, D. Acidity and Basicity in Zeolites. *Studies in Surface Science and Catalysis*. **1991**,*65* , 157-169 .

(34) de Lima, A. L.; Ronconi, C.M.; Mota, C. J. Heterogeneous Basic Catalysts for Biodiesel Production. *Catalysis Science & Technology*. **2016**, *6*, 2877-2891.

(35) Inaki, Y.; Kajita, Y.; Yoshida, H.; Ito, K.; Hattori, T. New Basic Mesoporous Silica Catalyst obtained by Ammonia Grafting. *Chemical Communications*. **2001**, 2358-2359.

(36) Verboekend, D.; Keller, T. C.; Mitchell, S.; Pérez‐Ramírez, J. Hierarchical FAU‐and LTA‐Type Zeolites by Post‐Synthetic Design: A New Generation of Highly Efficient Base Catalysts. *Advanced Functional Materials*. **2013**,23,1923-1934.

(37) Ni, X.; Xiang, M.; Fu, W.; Ma, Y.; Zhu, P.; Wang, W.; He, M.; Yang, K.; Xiong, J.; Tang, T. Direct Synthesis of Mesoporous Zeolite ETS-10 and Ni-ETS-10 with Good Catalytic Performance in the Knoevenagel Reaction. *Journal of Porous Materials* .**2016**, *23*, 423-9

(38) Xiang, M.; Ni, X.; Yi, X.; Zheng, A.; Wang, W.; He, M.; Xiong, Jing; Liu, T.; Ma, Y.; Zhu, P. Preparation of Mesoporous Zeolite ETS‐10 Catalysts for High‐Yield Synthesis of α, β‐Epoxy Ketones. *ChemCatChem*. **2015**, 7, 521-225.

(39) Yutthalekha, T.; Suttipat, D.; Salakhum, S.; Thivasasith, A.; Nokbin, S.;Limtrakul, J.; Wattanakit, C. Aldol Condensation of Biomass-Derived Platform Molecules Over Amine-Grafted Hierarchical FAU-Type Zeolite Nanosheets (Zeolean) Featuring Basic Sites.*Chemical Communications*. **2017**, *53*, 12185-12188.

(40) Thomas, M.; Nicolaos, A., Use of Caesium-exchanged Faujasite Type Zeolites for Intense Desulphurization of a Gasoline Cut.US Patent, No. 7,435,337 B2 , Oct.14, **2008**.

(41) Sooknoi, T.; Danuthai, T.; Lobban, L.L.; Mallinson, R.G.; Resasco, D.E. Deoxygenation of Methylesters over CsNaX. *Journal of Catalysis*. **2008**, *258*, 199-209.

(42) Breck, D.W.; Flanigen, E.M., Molecular Sieves, Society of Chemical Industry, London , **1968** 47.

(43) Baerlocher, C.H.; Meier, W.M.; Olson, D.H. (Eds.), Atlas of Zeolite Framework Types, 5th Revised Edition, Elsevier, **2001**.

(44) Atapour, M.; Kariminia, H.-R. Characterization and Transesterification of Iranian Bitter Almond Oil for Biodiesel Production. *Applied Energy*. **2011**, *88* , 2377-2381.

(45) Churasia, A.; Singh, J.; Kumar, A. Production of Biodiesel from Soybean Oil Biomass as Renewable Energy Source. *Journal of Environmental Biology*. **2016**, *37*, 1303.

(46) Gelbard, G.; Bres, O.; Vargas, R.M.;Vielfaure, F.;Schuchardt, U. F. ^{1} H Nuclear Magnetic Resonance Determination of the Yield of the Transesterification of Rapeseed Oil with Methanol *Journal of American Oil Chemists' Society*. **1995**, *72*, 1239-1241.

(47) Cychosz, K. A.; Guillet-Nicolas, R.; García-Martínez, J.; Thommes, M. Recent Advances in the Textural Characterization of Hierarchically Structured Nanoporous Materials. *Chemical Society Reviews.* **2017**, *46*, 389-414.

(48) Serrano, D.; Aguado, J.;Escola, J. Hierarchical Zeolites: Materials with Improved Accessibility and Enhanced Catalytic Activity. *Catalysis*. **2011**, *23*, 253-283.

(49) MacKenzie,K.J.D.;Smith,M.E., Multinuclear Solid-State Nuclear Magnetic Resonance of Inorganic Materials, Elsevier, **2002**.

(50) Engelhardt, J.; Szanyi, J.;Valyon, J. Alkylation of Toluene with Methanol on Commercial X Zeolite in Different Alkali Cation Forms. *Journal of Catalysis*. **1987**, *107*, 296-306.

(51) Concepcion-Heydorn, P.;Jia, C.;Herein, D.;Pfänder, N.;Karge, H.G.;Jentoft, F.C. Structural and Catalytic Properties of Sodium and Cesium Exchanged X and Y Zeolites, and Germanium-Substituted X Zeolite. *Journal of Molecular Catalysis A: Chemical*. **2000**, *162*, 227-246.

(52) Scokart, P.O.;Rouxhet, P.G. Characterization of the Basic Properties of Sodium Exchanged Zeolites through the Infrared Study of Pyrrole Adsorption. *Bulletin des Sociétés Chimiques Belges* . **1981**, *90*, 983-984.

(53) Barthomeuf, D. Conjugate Acid-Base Pairs in Zeolites. *The Journal of physical chemistry*. **1984**, *8*, 42-45.

(54) Sánchez-Sánchez, M.; Blasco, T. Characterization of Zeolite Basicity using Probe Molecules by Means of Infrared and Solid State NMR Spectroscopies. *Catalysis Today*. **2009**, *143*, 293-301.

(55) Uvarova, E.B.; Kustov, L.M.; Kazansky, V.B. Basicity of Zeolites: IR-Spectroscopic Study using Adsorbed Molecular Probes. *Studies in Surface Science and Catalysis*. **1995**, *94*, 254-261.

(56) Muciño, G.E.G.;Romero, R.;Garcia-Orozco, I.;Serrano, A.R.;Jiménez, R.B.;Natividad, R. Deactivation Study of K_2O/NaX and Na_2O/NaX Catalysts for Biodiesel Production. *Catalysis Today*. **2016**, *271*,220-226.

(57) Yuan, H.;Yang, B.;Zhu, G. Synthesis of Biodiesel using Microwave Absorption Catalysts *Energy and Fuels*. **2008**, *23*,548-552.

(58) Tangy, A.; Pulidindi, I.N.;Gedanken, A SiO_2 Beads Decorated with SrO Nanoparticles for Biodiesel Production from Waste Cooking Oil using Microwave Irradiation. *Energy and Fuels*. **2016**, *30*, 3151-3160.

(59) Leclercq, E.;Finiels, A.;Moreau, C. Transesterification of Rapeseed Oil in the Presence of Basic Zeolites and Related Solid Catalysts. *Journal of the American Oil Chemists' Society*. **2001**, *78*, 1161-1165.

(60) Suppes, G.J.;Dasari, M.A.;Doskocil, E.J.;Mankidy, P.J.;Goff, M.J. Transesterification of Soybean Oil with Zeolite and Metal Catalysts. *Applied Catalysis A: General*. **2004**, *257*, 213-223.

(61) Musa, I.A. The Effects of Alcohol to Oil Molar Ratios and the Type of Alcohol on Biodiesel Production using Transesterification Process. *Egyptian Journal of Petroleum*. **2016**, *25*, 21-31.

TOC Graphic

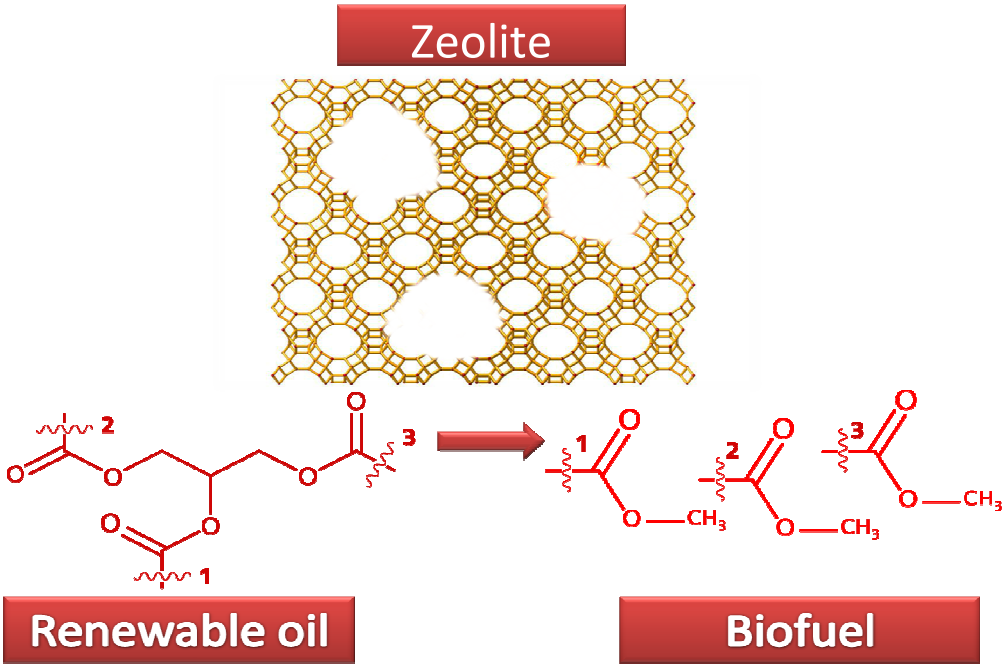

Zeolite

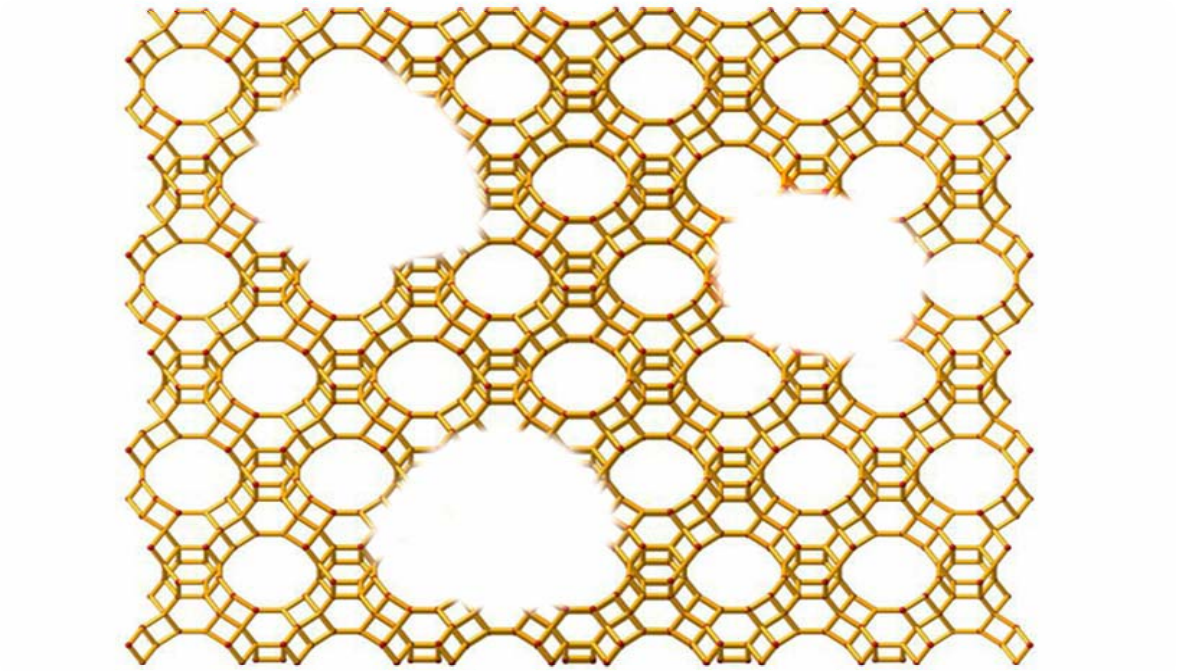

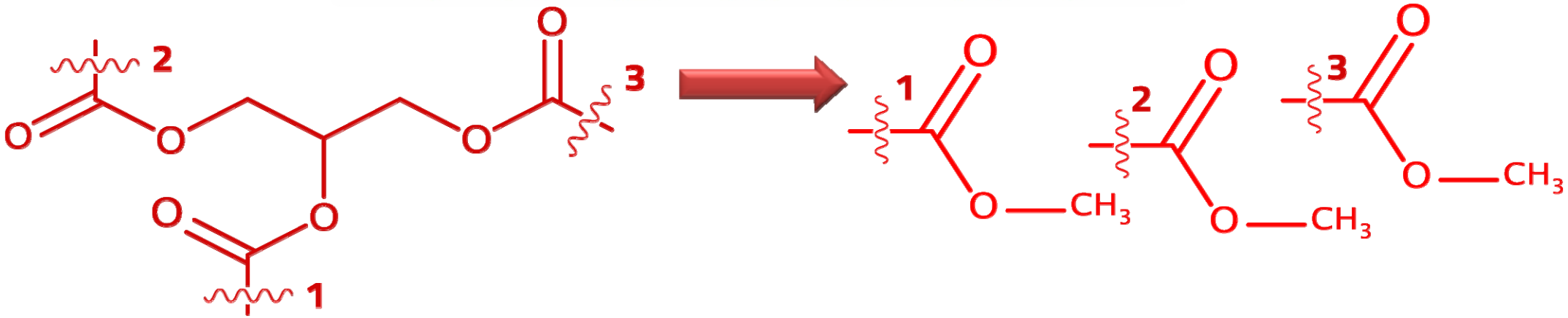

Renewable oil

Biofuel